Near-surface seismic imaging: refraction tomography and reflection imaging

David C. Henley, Robert A. Birch, and Robert R. Stewart

ABSTRACT

Near-surface shallow seismic imaging techniques have been under development for a number of years and are used in an increasing number of applications. Concurrently, archaeological investigation has made increasing use of various geophysical techniques, principally potential field and electrical methods, to detect subsurface anomalies of potential archaeological interest. To date, however, seismic methods have received little attention for use in archaeological investigation. This chapter describes a recent application of two seismic imaging techniques at Ma'ax Na, a Mayan temple site in Belize. Three intersecting shallow seismic lines were acquired at this site. Analysis of the data is incomplete, but early results include reflection images for all three lines, as well as tomographic images obtained by applying the turning-ray model to first break time picks. All the images appear to tie reasonably well at intersection points, but for the shallowest section of the earth, the tomographic images appear to contain the most useful information for archaeological purposes.

INTRODUCTION

While seismic methods have not been used much in archaeology, other geophysical technologies have a history of at least partial success at archaeological sites, in particular, ground-penetrating radar (GPR). Because of its sensitivity to conductive or resistive boundaries in the subsurface, GPR can be successfully used to locate void spaces and regions of disturbance that interrupt conductive layers like the water table. On the other hand, local soil conditions often preclude the use of GPR, which loses its penetration rapidly in the presence of conductive groundwater and/or clay minerals. It is believed that shallow seismic methods can provide a possible alternative for some kinds of targets. The knowledge gained from working with shallow, high-resolution seismic data in the archaeological context will improve understanding of near-field seismic wave propagation and provide insight into the nature and structure of the earth's near-surface, which often contributes disproportionately to the imaging problems with more conventional seismic reflection data. Such knowledge will be increasingly important as acquisition technology moves toward an ever-expanding number of discrete channels recording the output of single geophones spaced at ever-decreasing distances

High-resolution seismic techniques have been increasingly applied to the shallowest part of the earth in pursuit of a number of objectives, such as delineation of the weathered layer, mapping of shallow coal seams, investigating soil structure for geotechnical purposes, etc. See, for example, Steeples et al. (1985; 1986; 1988) or Miller et al. (1988) for early work in shallow seismic methods. Growing interest in the field is indicated by the fact that the most recent SEG convention (Salt Lake City, 2002) featured no fewer than four sessions on near-surface geophysics, including seismic methods. One seismic objective which has been suggested, but not often pursued, is that of locating near-surface

anomalies of interest to archaeologists, in order to intelligently plan expensive excavation. Previous efforts to use seismic imaging have been described by Henley (2000; 2001) for Chan Chich, a Mayan temple site in Belize. That work identified some of the difficulties involved in such seismic work and provided clues for improving techniques. Each successive archaeological seismic survey has built upon information obtained during previous efforts, to guide both acquisition and processing of subsequent surveys. The work reported here is the third archaeological seismic survey performed in as many years and reflects the improved knowledge.

SHALLOW SEISMIC TECHNIQUES

Conventional seismic survey methods are usually not suited to exploring the very near-surface for several reasons. Because they are intended to image regions of the subsurface hundreds or thousands of metres in depth, conventional seismic acquisition systems use very energetic sources and large numbers of widely spaced geophones distributed over considerable distance on the earth's surface. A field crew consisting of several specialists and a number of casual labourers is required to deploy such systems. This makes them far too expensive and unwieldy to use for smaller scale surveys; and there are usually practical difficulties in deploying conventional geophone strings and cables over the very short distances typical of shallow surveys. Consequently, shallow surveys are usually performed with portable seismic recorders having a limited number of channels (60 is a typical number), single geophones, and relatively weak (and cheap) surface sources. Surveys on this scale can be performed rapidly by as few as two people, so that acquisition costs and time are not greatly different than for a GPR survey.

A consequence of the limited number of channels available for shallow seismic recording is that often either the range of source-receiver offset distances is limited, or the data redundancy (fold) is small. The use of a surface source creates special problems, since such sources often excite large amplitude surface and guided wave modes and refractions. These may be analysed for their own unique information, but they must be significantly attenuated in order to image reflections. Since the fold in shallow surveys is often insufficient for the stack process to remove coherent noise, pre-stack noise attenuation is usually necessary. The shallowest reflections, especially, are often obscured by near-surface refractions, which must be removed in order to analyse the reflection moveout prior to NMO correction and stacking. For the shallowest interfaces, as well, a reflection can often be observed on only the two or three nearest offset traces, so that stack fold in reflection imaging is particularly low.

PREVIOUS RESULTS

Among the phenomena observed in the data from the first two archaeological surveys at Chan Chich (Henley, 2000; 2001) was the presence, at comparable amplitudes, of both the PP particle motion and the PS particle motion on either the vertical geophone channels or the horizontal inline geophone channels. This implies that only one of the components need be measured in order to image both PP and PS energy at this particular survey site. Other phenomena of note are the very large Vp/Vs ratio (at least 5:1) implied by the greatly different NMO velocities required to stack the PP reflection image and the

PS conversion image (300 m/s and 75 m/s, respectively), as well as the relatively much greater vertical resolution of the PS image.

A dramatic increase in velocity of the near-surface material in the 2001 Chan Chich survey compared to the 2000 survey on the same profile led to a much shallower PP reflection image for the bedrock at the site, which meant that this reflection was present on even fewer traces than in the 2000 survey, and its image correspondingly less trustworthy in spite of its coherence and amplitude. This sparsity of reliable reflection signal was the motivation for a trial of turning-ray tomography, using the first break pick times, as an alternate way to image the near-surface. In this approach, a single transit time is picked on each of the 400 seismic traces in the survey. Each transit time is then associated with a model transit time obtained by tracing a smoothly curving ray between appropriate source and receiver points in a laterally homogeneous, vertically increasing velocity model. The set of transit time differences between observed and modelled traveltimes is then used to estimate a velocity variation in each model cell which reduces the rms transit time differences for all rays traversing the cell. The velocity variations, superimposed on the starting model, comprise the tomographic image. For the Chan Chich site, it was found that the tomographic image showed a distinct low-velocity anomaly that was exactly coincident with a weakening of the corresponding reflection (which images *differential* velocity across boundaries). The close correspondence of these two images, derived from essentially independent measurements increased confidence in the existence of a low-velocity anomaly of archaeological interest at Chan Chich (Henley, 2001). The result from turning-ray tomography also demonstrated the potential for this method in the shallowest part of the subsurface where reflections become problematic, as long as the structure of the near-surface conforms to the underlying model for turning-ray tomography (strongly increasing velocity with depth, with no velocity inversions). For the reflection method to work in the shallow earth, anomalies must have sharp horizontal velocity boundaries, since reflection images in the shallow section use mainly vertically travelling seismic energy. Tomography, on the other hand, detects anomalies with significantly different velocity, but does not require sharp boundaries. Furthermore, the seismic energy used in tomography travels mainly horizontally, making its raypath geometry more favourable for detection of lateral velocity variations than that of seismic reflections.

Among the lessons learned about acquisition of shallow seismic data at the Chan Chich site were the fact that a single sledgehammer blow as a source appeared to be better than the stacking of multiple blows, that 1-metre station spacing is adequate for imaging in the upper 10-20 metres when acquisition channels are limited, and that the seismic properties of the near-surface can change dramatically from year to year likely due to local precipitation, making time-lapse surveys problematic.

MA'AX NA 2002

Like Chan Chich, the Ma'ax Na site is a Mayan temple complex in Belize. Archaeological objectives include identifying buried anomalies in the 'plaza' region of the complex which might bear early examination. One possibility at this site is remnants

of earlier structures, which, being stone, are expected to be higher in velocity than the rubble and soil in which they may be buried.

Based on lessons learned at Chan Chich, a seismic survey was designed for Ma'ax Na which comprised three intersecting seismic lines, one north-south, the others east-west in orientation. Figure 1 shows the layout of the survey relative to structures previously identified on the perimeter of the plaza area. Because of the line intersections, character and traveltime ties at those intersections between images generated for each seismic profile should help confirm that the imaging methods are appropriate and boost confidence in any anomalies observed.

The N-S plaza line at Ma'ax Na (designated N-S-1) was 60 stations long, with 1 metre station spacing. The length was dictated by the channel capacity of the recording instrument and the number of geophones available. The survey technique was to carefully plant the 60 geophones, then to place 61 source points (sledgehammer impact points) between the stations, starting from 0.5 metres off the beginning of the spread and ending 0.5 metres off the end. This 'shooting through the spread' has become a common technique not only for shallow seismic surveys, but also for relatively short conventional surveys. Advantages of the technique, in addition to the logistical one of leaving the spread in place, are the comparable spatial sampling of source and receiver gathers (1 metre in both cases) and the decoupling of any short wavelength source and receiver statics (0.5 station offset between any source point and the two nearest geophone stations). Disadvantages include the relatively large fold variation along the line as well as the variation of offset distribution within the CDP gathers. The southernmost of the two E-W lines (designated E-W-1) is 51 stations in length, and its station 28 coincides with N-S-1 station 31; while the other E-W line, E-W-2, is 41 stations long with its station 22 coincident with N-S-1 station 47. As with N-S-1, station spacing on both E-W-1 and E-W-2 is 1 metre, and source points are between the stations.

Figure 2 shows four typical source gathers from line N-S-1. As is common with shallow seismic surveys, reflections are not readily visible on these gathers, which exhibit several modes of coherent noise. In addition, the shallow refraction events show evidence of significant statics, hinting at significant velocity variations in the near-surface. Source gathers from lines E-W-1 and E-W-2 are essentially similar except for the number of traces. In spite of the relatively high stack fold for these lines (implied by the number of stations), coherent noise attenuation is the first step in processing for each of the lines. Radial trace domain filtering (Henley, 1999; 2000) is particularly effective in attenuating linear noise overlying shallow reflections with similar moveout, and Figure 3 shows the gathers of Figure 2 after 4 passes of radial trace filtering. While linear events corresponding to shallow refractions are still present, fragments of shallow reflections (10 ms and 70 ms) can be seen on the smaller offset traces of some of the gathers (only two or three traces for the 10 ms reflection). Subjecting the gathers to Gabor deconvolution (Margrave et al., 2002) sharpens the image of these reflections and reveals other shallow reflections (40 ms), as shown in Figure 4. Rough estimates of NMO velocities can be made from the reflection fragments on these gathers and used for NMO correction as well as post-stack Kirchhoff migration. Stretch muting after NMO correction is used to effectively eliminate most of the shallow refraction arrival, at offsets greater than 10

metres, not removed by the radial trace filtering. A final pass of Gabor deconvolution to further whiten the image completes the processing for this initial reflection imaging attempt. At this point, no attempt has been made to determine or apply statics. Figure 5 shows the deconvolved, migrated stack image for line N-S-1, with the intersections of lines E-W-1 and E-W-2 marked. Of interest is the most prominent shallow event at about 10 ms. Because of the careful filtering and muting aimed at removal of refractions and other dipping linear events on the source gathers, the event is composed mostly of reflection energy from the interface between surface rubble/soil zone and the more competent bedrock. A less prominent and less regular interface appears at about 40 ms and may mark a transition of some kind within the massive carbonate bedrock (from karst to non-karst, perhaps?), while an even less regular reflection appears at 70 ms. While a weakly anomalous zone appears in the shallow reflection from about station 35 to 45, the fact that fewer than 10 % of the traces in the survey contribute to this reflection diminishes confidence in the details of this reflection. Processing of these data continues and will include an attempt to determine and remove statics

The local geology makes Ma'ax Na a candidate for turning-ray tomography. The line N-S-1 has 3660 traces, and thus the potential for great redundancy in first break tomography. The technique chosen for picking the first breaks was the threshold based automatic picker associated with the 'Trace display' operation in ProMAX. This operation generated the first set of picks, which were edited later by hand. In the first attempt at picking, it appeared that more than half of the automatic picks were good, most of the mispicks appearing at the longer offsets. The picks originating from the nearest 50% of the traces of each source gather appeared to have fewer than 10% mispicks.

Figure 6 shows the starting velocity model for the turning-ray tomography, based on interval velocities from NMO velocities. In the version of turning-ray tomography used here, raypaths traced through the starting model are used for all iterations of the tomographic inversion without being updated or retraced; the assumption is that the velocity changes occurring during the tomographic procedure, to first order, do not significantly move the raypaths. Using the image from the initial tomography pass as a new starting model is seldom successful because of the instability of the raytracing procedure through velocity models that are not carefully smoothed and conditioned. Figure 7 shows the tomographic image of the velocity structure of the near-surface based on raw (unedited) first break picks. Because most of the mispicks occur on the farthest offset traces, the deepest half of the tomographic image is the least reliable. Three distinct velocity anomalies can be seen in the upper 10 metres of this image, the left-most one (about 15 metres from the south end of the line) quite faint.

Visual inspection of the time picks revealed no source-consistent or receiver-consistent patterns of mispicks, which can lead to artifacts along the upper edge of the image, and it is unlikely that anomalies in the interior of the image are due to mispicks. To test that assertion, Figure 8 shows the tomographic image resulting from using the same starting model (Figure 6), but using hand-edited first break picks to greatly reduce the number of mispicks. Note that the images are similar and that the anomalies present in Figure 7 also occur in Figure 8, but with somewhat different contrast and shape. It is interesting to note that all anomalies are 'hard' or high-velocity zones (with respect to the

starting model), and that two of them are each intersected by a cross line. Figure 9 is a re-scaled version of the reflection image at roughly the same scale as the tomographic images in Figures 7 and 8. While some correspondence can be seen between the images, the information on the reflection image is insufficient to interpret the presence of the three 'hard' anomalies. There are faint hints of their presence, nevertheless; such as the disturbed zone just beneath the shallow reflection (6 metres), and the possible 'pull-up' of segments of the 16 metre reflection beneath the anomalies. A precaution for interpreting tomographic images is that 'hard' and 'soft' are only relative to the starting model, not necessarily to the actual earth. Also, the raypath density of the starting model can leave a 'footprint' on the image that should be disregarded in interpretation. Some evidence of the turning-ray footprint can be seen in all the tomographic images presented here.

The same processing flow and parameters were used to process lines E-W-1 and E-W-2, both for reflection imaging and tomographic imaging. Figure 10 is the reflection image of line E-W-1 with the intersection with line N-S-1 marked. Comparison of this line with line N-S-1 (Figure 5) at the intersection shows good agreement between event timing and amplitude. Turning-ray tomography using the 2550 raw first break picks from this data set with the starting model of Figure 6 yields the image in Figure 11, shown with the N-S-1 line intersection indicated. As with line N-S-1, prominent 'hard' anomalies appear in the shallow portion of the image. Interestingly, the anomaly shown just touching the left side of the N-S-1 line intersection ties a similar anomaly in Figure 7 and is likely due to the same 'hard' object. Figure 12 is a re-scaled reflection image for this line. Again, some correspondence can be seen between details of the reflection image and the anomalies on the tomographic image (particularly the interrupted events bordering the prominent 'hard' anomaly between 6 and 10 metres of depth. Once again, however, the tomographic image provides a much better indication of the anomalies than the reflection image. First break picks for this line have yet to be edited for further imaging.

The reflection image for line E-W-2 is shown in Figure 13, with the N-S-1 line intersection marked. Again, comparison with Figure 5 in the vicinity of the line tie shows good agreement between event timing and amplitude between the two images. The tomographic image resulting from 1640 raw first break picks is shown in Figure 14 and the re-scaled reflection image in Figure 15. The tomographic image contains an elongated 'hard' anomaly that ties closely with the anomaly on N-S-1. The two images imply that N-S-1 crossed the anomalous zone along the short dimension, while E-W-2 encountered the same zone along its length. Such an elongated anomaly could represent a buried portion of an old structure. A comparison of Figures 14 and 15 shows very little evidence, on the reflection image, of the anomalous 'hard' zone seen with tomography. Again, as with the previous two lines, the tomographic image seems to be a better detector of a velocity anomaly than the reflection image. As is the case with line E-W-1, the first break picks on this line have yet to be edited for further imaging attempts.

DISCUSSION AND CONCLUSIONS

In addition to observations made about the two earlier seismic archaeology experiments at Chan Chich (Henley 2000; 2001), the survey at Ma'ax Na helps to confirm the following:

- Current field technique seems adequate: single 1-C or 3-C phones with 1-metre spacing (closer spacing could be useful if obtainable); single sledgehammer blows between the receiver stations; stationary geophone spread, moving source point from one end of the spread to the other.

- Reflection imaging of the shallowest interfaces (< 10 metres) is difficult because reflections are present on only a small number of short-offset traces for any shot gather; and those reflections present are usually masked by strong coherent noise which must be strongly attenuated before imaging the reflections.

- Reflection imaging may not, in fact, be the best detector of the types of anomalies of interest to archaeologists in the very shallow subsurface. Their dimensions and shape can be near the lateral resolution limits for seismic reflection methods, and may lead only to less easily interpreted diffractions. Also, the anomalies may not exhibit a sharp boundary, but only a velocity gradient, making them unresponsive as reflectors.

- It is often not clear from particle motion detected at the surface whether a coherent event is a PP reflection or PS conversion. Moveout velocities are difficult to measure and may not provide sufficient discrimination.

- Turning-ray tomography from first break time picks, although fraught with its own uncertainties due to the approximations in the method, seems to provide clear images of velocity anomalies in the near-surface at the scale of interest to archaeologists. To use this technique, however, the background velocity structure of the near-surface must be a simple one, however, with velocity strictly increasing with depth.

- First break picks can generally be obtained more readily from any seismic data set than reflections, and often with far greater redundancy. Furthermore, no processing, such as coherent noise attenuation, is necessary prior to picking first breaks; and mode identification is not required, since for the type of velocity structure for which turning-ray tomography is valid, the first arriving energy will always be compressional.

These observations lead to the conclusion that perhaps the first and best thing that should be done with any archaeological seismic data set is to pick first breaks and perform tomography. The analysis and processing of the bulk of the data to form reflection images can involve much trial processing and some mode interpretation, and may not ultimately be successful in attaining the objective of convincingly delineating archaeological anomalies. As an example of what may be possible, Figure 16 shows the ‘hard’ anomalies detected by turning-ray tomography posted on the Ma’ax Na site map, with the weight of the contour indicating anomaly reliability. Work on the Ma’ax Na data is still in its early stage and will continue in order to learn as much about the data and the method as possible. A processing strategy for imaging shallow seismic data is beginning to emerge and should continue to solidify with continued effort.

ACKNOWLEDGEMENTS

The author wishes to acknowledge the support of the sponsors of CREWES and various staff members for discussion.

REFERENCES

Henley, D.C., 2000, Harsh imaging techniques for shallow high-resolution seismic data, CREWES Research Report, Volume 12.

Henley, D.C., 2001, New imaging results at the Chan Chich archaeological site, CREWES Research Report, Volume 13.

Margrave, G.F., Lamoureux, M.P., and Henley, D.C., 2002, Improvements to Gabor deconvolution, CREWES Research Report, Volume 14.

Miller, R.D., Steeples, D.W., Somanas, C. and Myers, P.B., 1988, Detecting voids in a 0.6 m coal seam, 7 m deep, using seismic reflection, 58th Ann. Internat. Mtg: Soc. of Expl. Geophys., Session:ENG1.7

Steeples, D.W., Knapp, R.W. and Miller, R.D., 1985, Field efficient shallow CDP seismic surveys, 55th Ann. Internat. Mtg: Soc. of Expl. Geophys., Session:ENG2.1.

Steeples, D.W. and Miller, R.D., 1986, Some shallow seismic reflection pitfalls, 56th Ann. Internat. Mtg.: Soc. of Expl. Geophys., Session:ENG1.1.

Steeples, D.W., Miller, R.D. and Brannan, M., 1988, Mapping bedrock as shallow as 4 m under dry alluvium with seismic reflections, 58th Ann. Internat. Mtg: Soc. of Expl. Geophys., Session:ENG2.2.

FIGURES

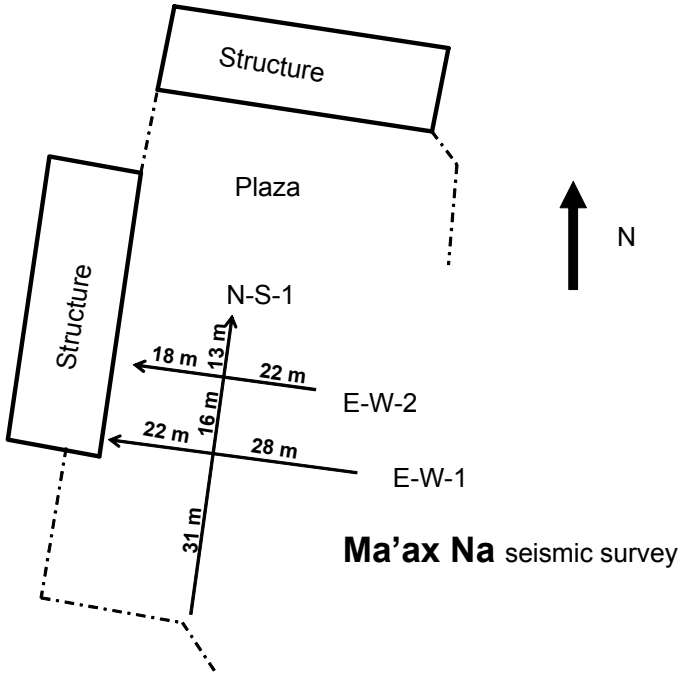

FIG. 1. Simplified site map of the Ma'ax Na archaeological site. Layout and dimensions of each of the three seismic lines is shown.

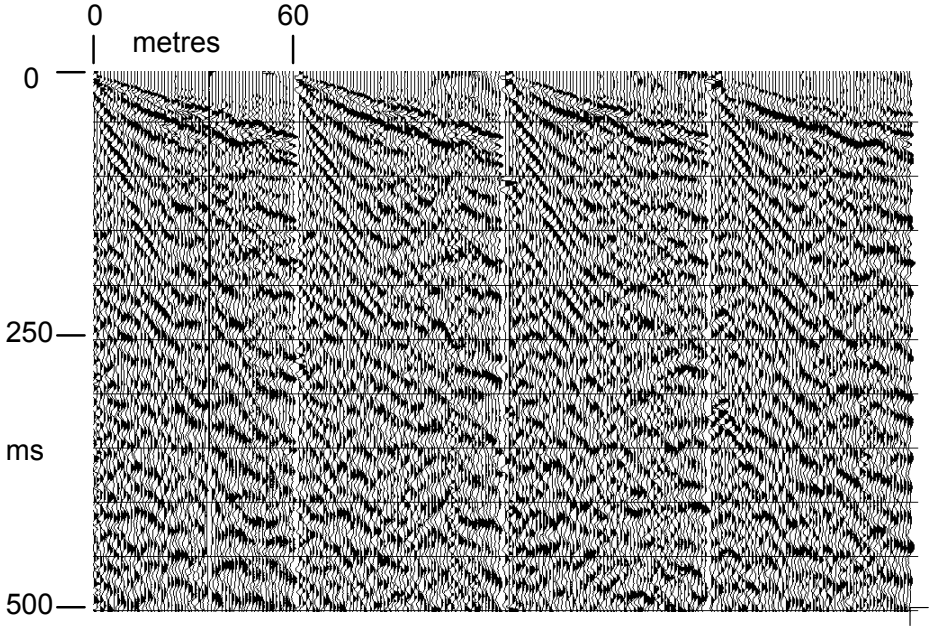

FIG. 2. Four shot gathers from line N-S-1 at Ma'ax Na. Reflections are masked by source-generated noise.

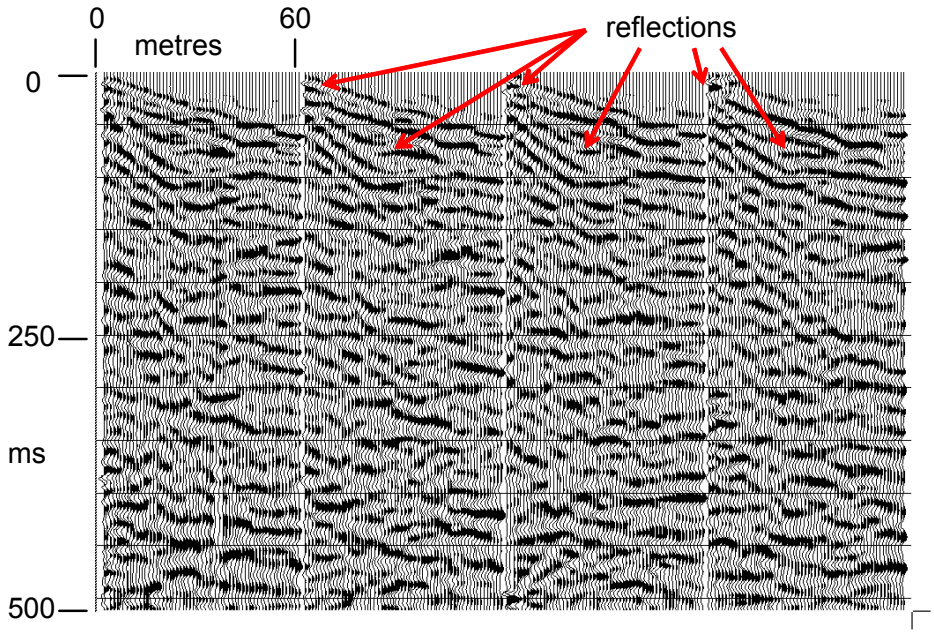

FIG. 3. Shot gathers after three passes of radial trace filtering. Linear noise still present, but reflections also visible.

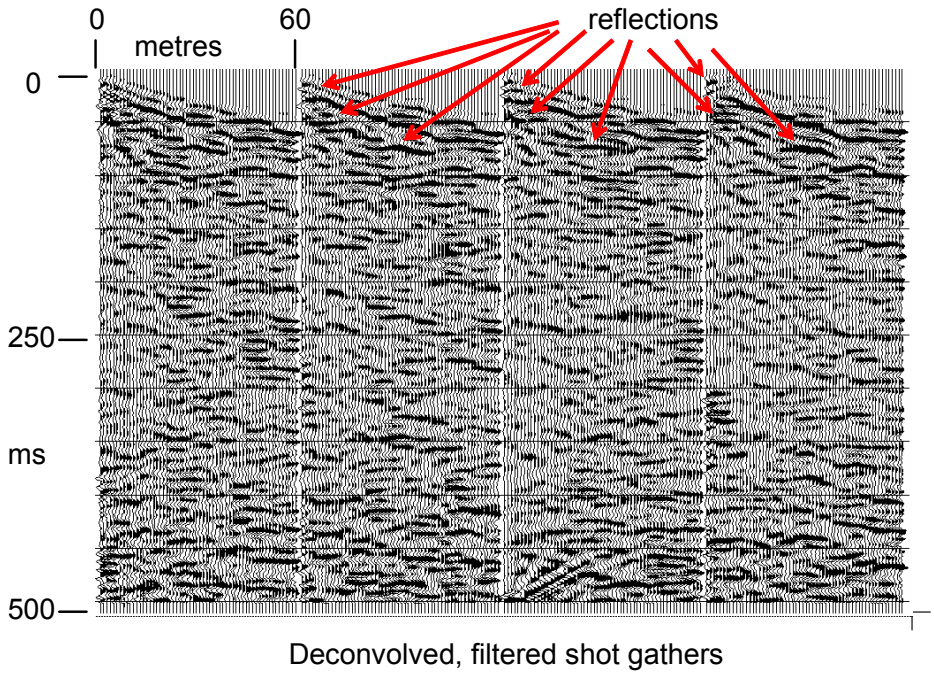

FIG. 4. Shot gathers after radial trace filtering and deconvolution with Gabor time-varying deconvolution.

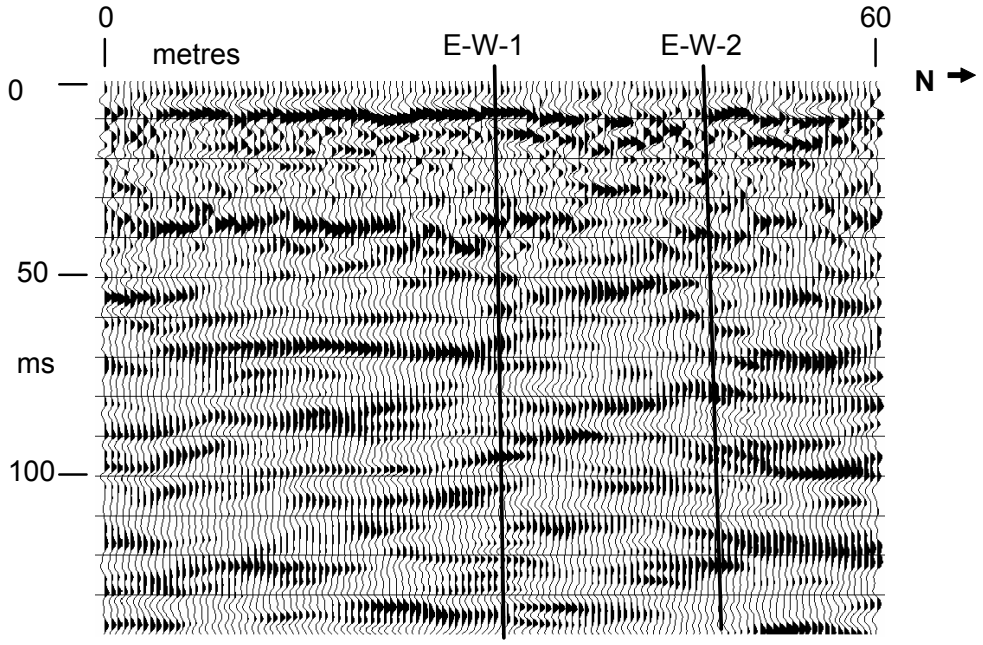

FIG. 5. Reflection image for line N-S-1.

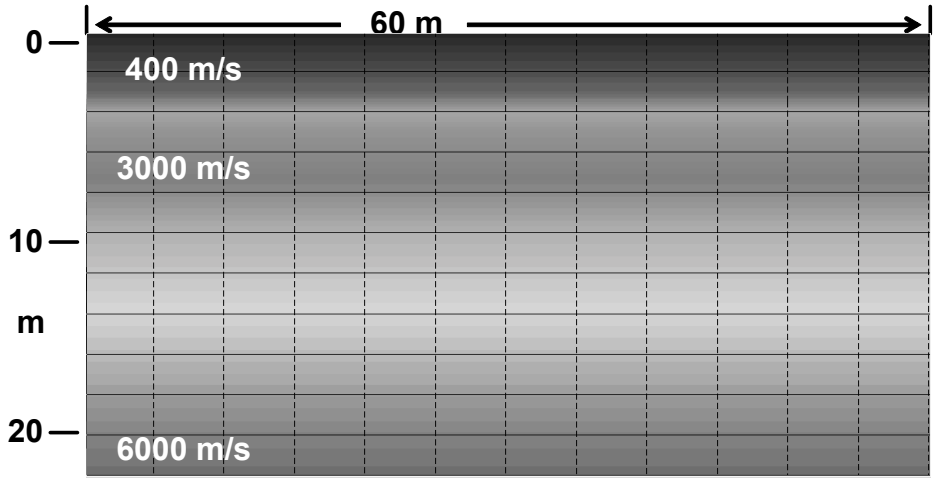

FIG. 6. Flat, smoothly varying velocity model used for starting model for turning-ray tomography.

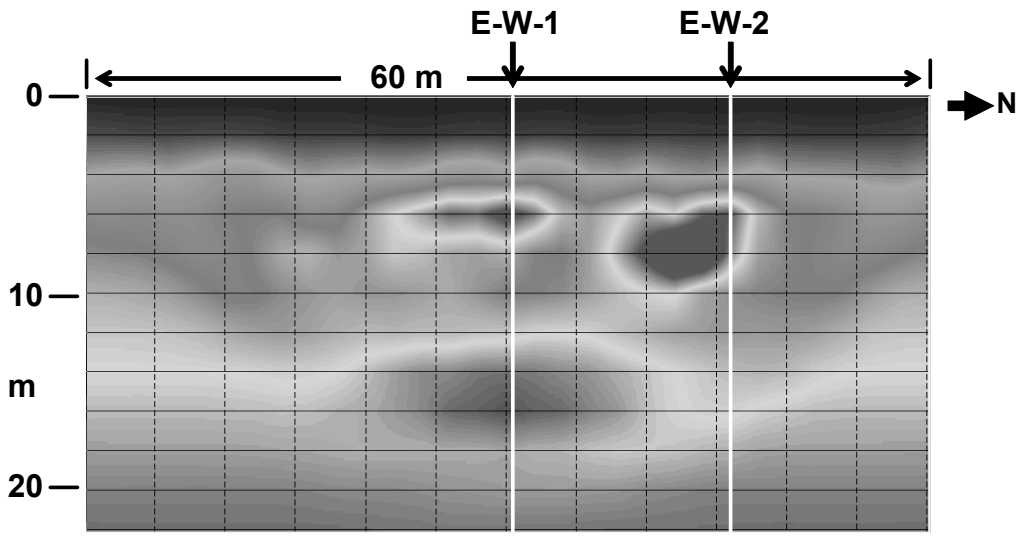

Turning ray tomographic image of Ma'ax Na line N-S-1

FIG. 7. Tomographic image of near-surface for line N-S-1. Image was created using starting model in Figure 6 and raw (unedited) first break picks on unfiltered shot gathers.

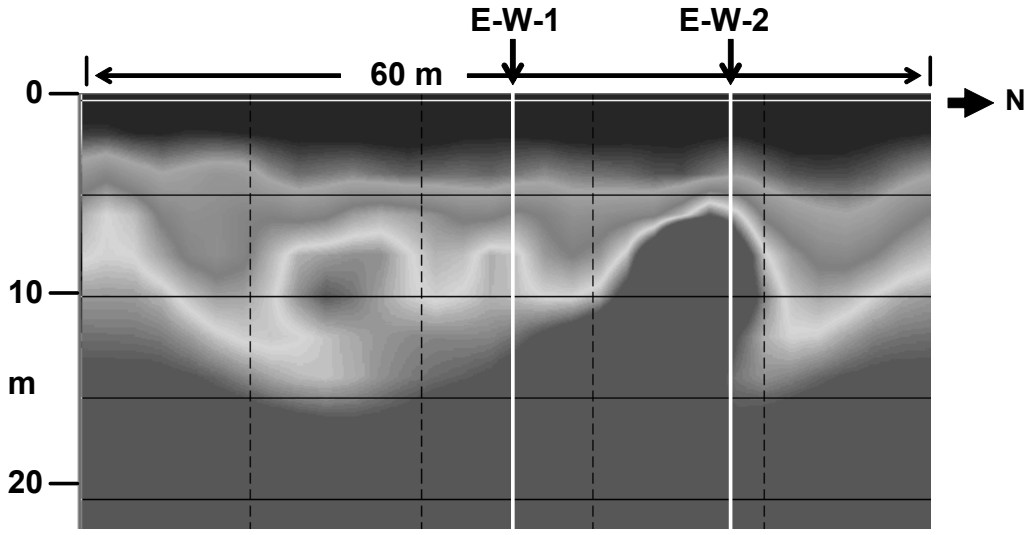

Turning ray tomographic image of Ma'ax Na line N-S-1

FIG. 8. Tomographic image for line N-S-1 using hand-edited first break picks. Anomalies differ in velocity contrast with background, compared to the image in Figure 7, but anomaly location is similar.

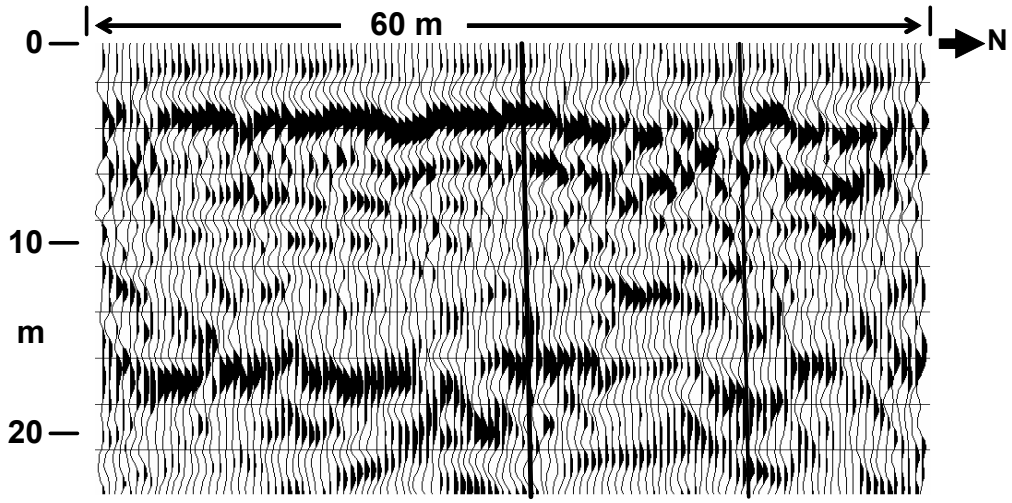

FIG. 9. Reflection image for line N-S-1, rescaled to approximately match the depth scale of Figures 6-8.

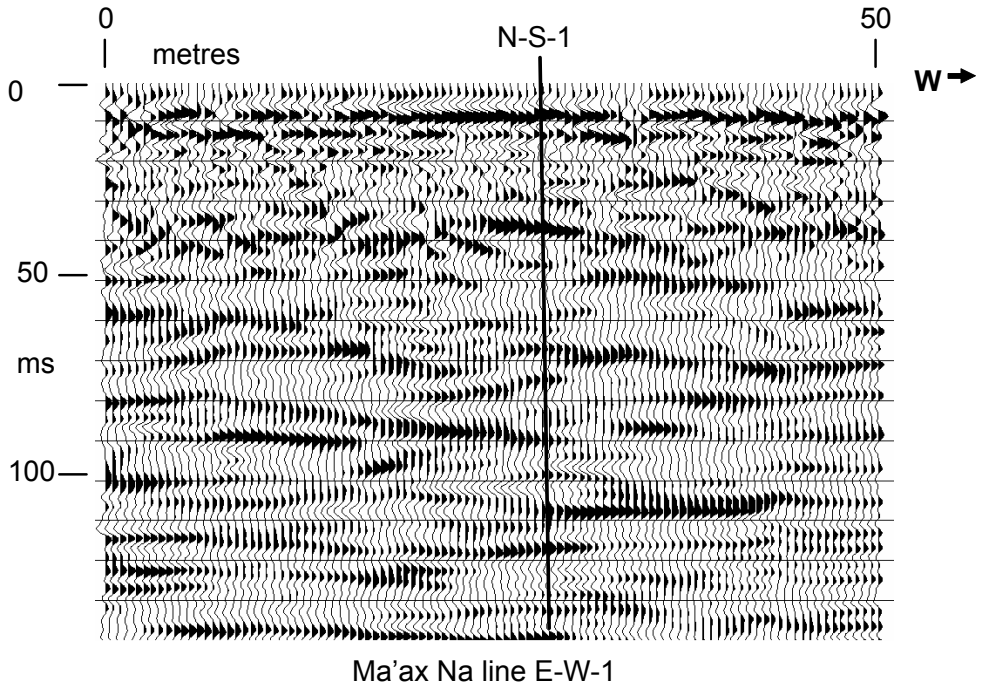

FIG. 10. Reflection image for line E-W-1.

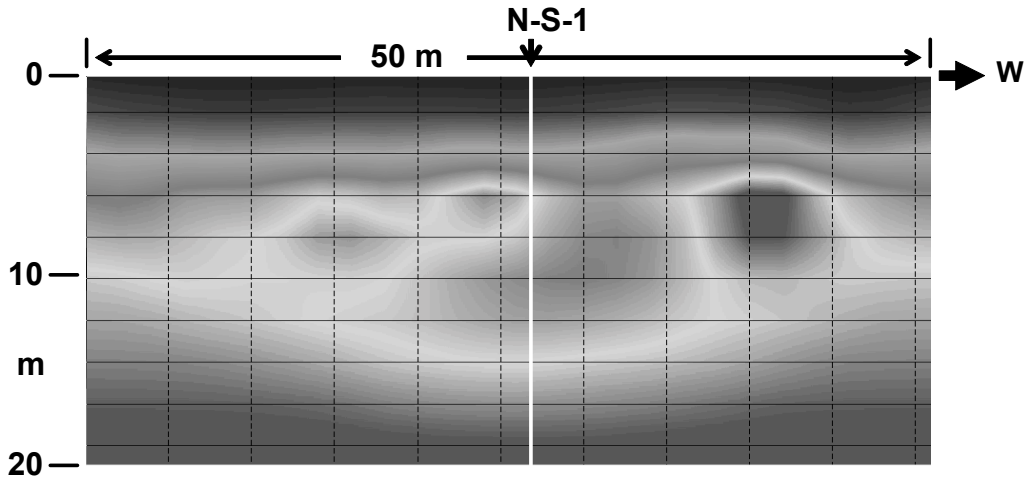

Turning ray tomographic image of Ma'ax Na line E-W-1

FIG. 11. Turning-ray tomographic image of near-surface for line E-W-1, created from starting model in Figure 6 and raw first break picks on unfiltered shot gathers.

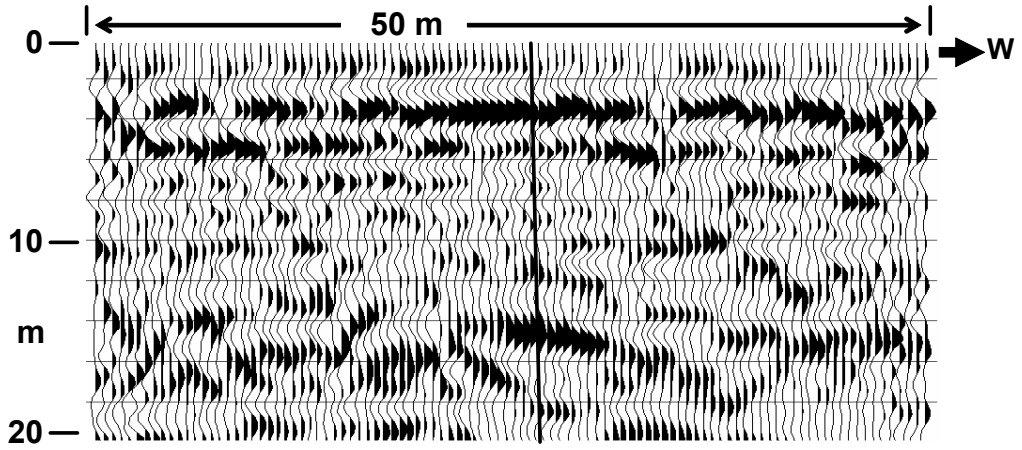

Expanded reflection image of Ma'ax Na line E-W-1

FIG. 12. Reflection image of line E-W-1, rescaled to approximately match depth scale of Figure 11.

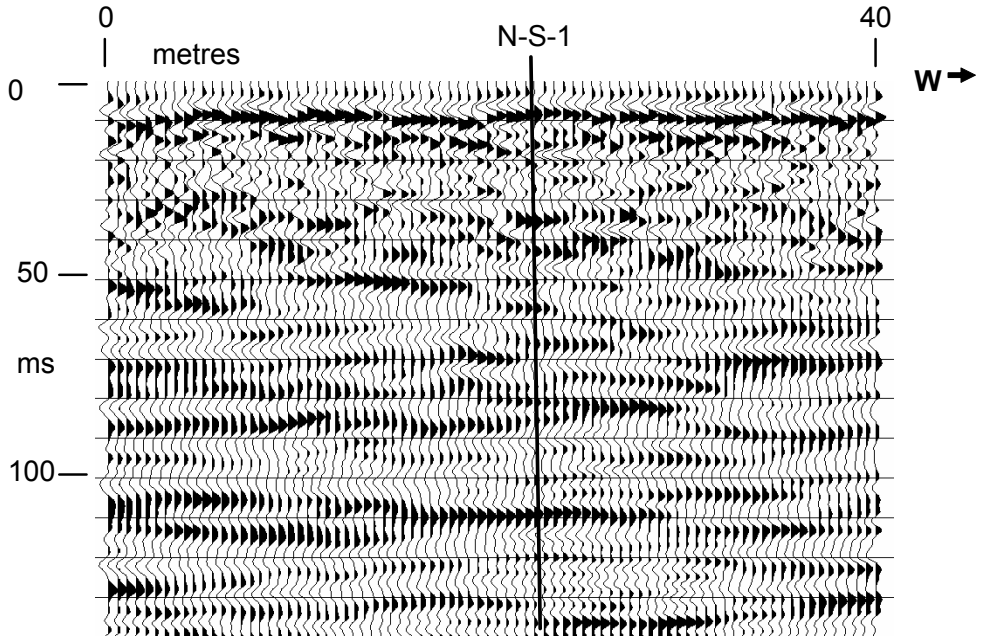

FIG. 13. Reflection image for line E-W-2.

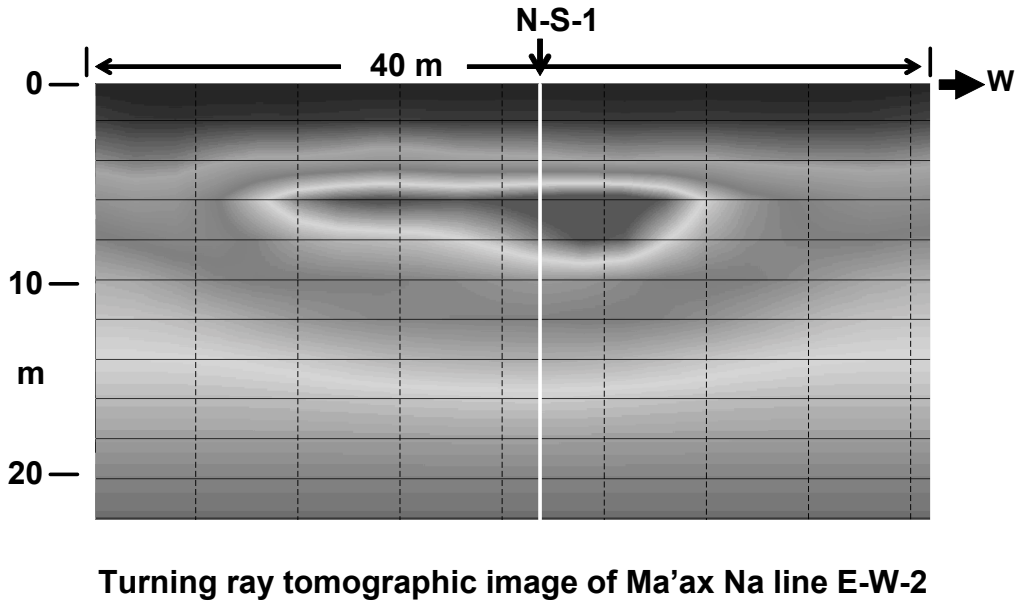

FIG. 14. Turning-ray tomographic image for line E-W-2, created from starting model in Figure 6 and raw first break times picked on unfiltered shot gathers.

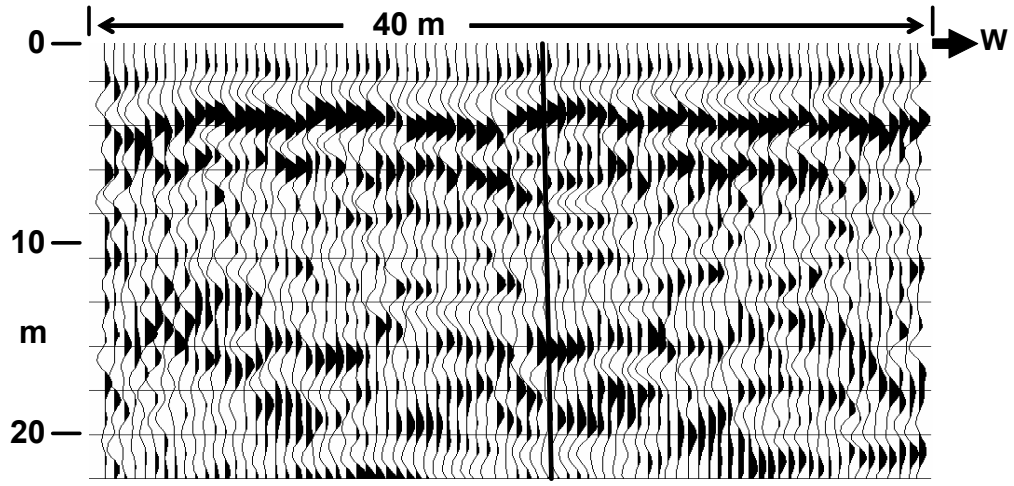

FIG. 15. Reflection image of line E-W-2, rescaled to approximately match depth scale of Figure 14.

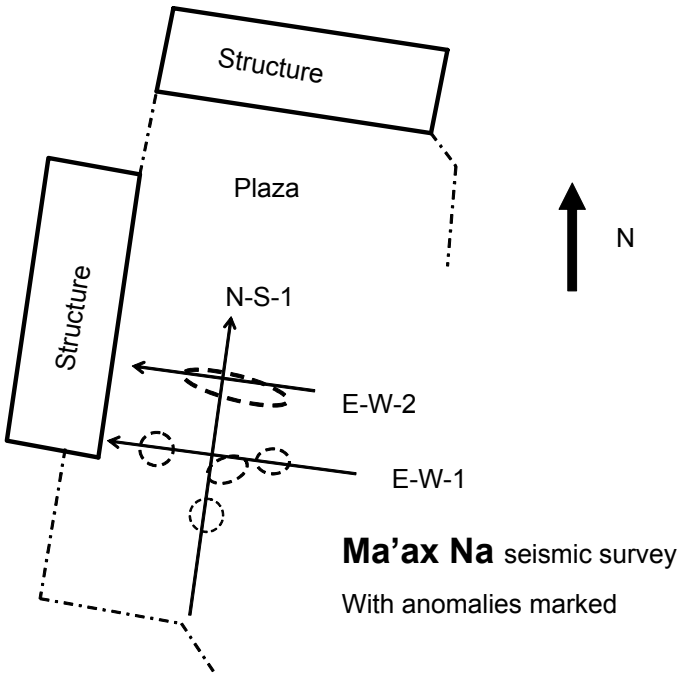

FIG. 16. Ma'ax Na site map showing location of 'hard' anomalies seen on tomographic images. More reliable anomalies indicated by heavier outlines.